IEEE Transactions on Nuclear Science, Vol.NS-22, No.3, June 1975

NUMERICAL SIMULATION OF THE ACCELERATION OF ION-LOADED ELECTRON RINGS*

A. C. Greenwald and M. P. Reiser

University of Maryland
College Park, Maryland 20742

Abstract

Numerical studies were performed to simulate the acceleration of ion-loaded electron rings by the magnetic expansion method. A finite-sized multi-particle code is used that computes particle-particle interaction forces directly and approximates conductive boundaries. Initial conditions are electron-ion rings in equilibrium, trapped in a magnetic mirror. On one side, the magnetic field is reduced in time, allowing the ion-loaded ring to move into a region of expansion acceleration. The calculations show that the use of a "squirrel-cage" type conductor inside the beam, which suppresses azimuthal magnetic image currents, assures sufficient axial focusing to retain the integrity of the ring.

1. Introduction

The work reported here represents a computer simulation of the initial acceleration of the ion-loaded ring in the University of Maryland Electron Ring Accelerator.[1] Its main objective was to provide some theoretical guidance for the design of the experiments that are planned after the expansion-acceleration coils have been installed.

Recent experiments in the existing facility have demonstrated the feasibility of forming an axially compressed toroidal beam by passing a hollow, cylindrical electron pulse through a cusped magnetic field.[2] After extension of the magnetic field downstream of the cusp, the electron ring will be trapped between two small coils with fast rise time which generate a time-dependent magnetic mirror field on top of the external static field.[1] Single-particle as well as collective-effect calculations by members of the Maryland ERA Group[3] have shown that such a trapping scheme, possibly combined with resistive-wall damping of coherent amplitudes,[4] should be feasible, and hardware design is presently in progress in collaboration with the Garching ERA Laboratory.

In the studies reported here, it is assumed that an ion-loaded electron ring has been formed in the fast-trapping system. We then investigate the opening of the trapping well on the downstream side and follow the ion-loaded ring as it moves into the region of magnetic expansion acceleration.

2. Geometry, Parameters and Method of Computation

Figure 1 shows the magnetic field configuration. There is a large, steady, externally created B_z which falls off slowly (10% in one meter) with axial distance. In the absence of other coils, this would provide for collective acceleration of protons of the order of 10 MeV/meter. On top of this field, the two pulsed coils provide a 10% (peak) perturbation to form a magnetic mirror. At time t = 0, an ion-loaded electron ring is assumed to exist at the minimum B_z in the well. The current in the second coil is taken as an exponentially decreasing function of time, with characteristic constant τ_c. The point of minimum B_z moves towards the right and eventually disappears. If τ_c is small, and the ions are very massive and/or the fraction f of ions is high, the electron ring can lag behind this point of minimum B_z. However, our numerical studies show that this does not necessarily disrupt the ring.

Figure 2 shows a model of the electron ring used in most of the computations. Initially, it has a square cross section in the r-z plane of about 1/2 cm by 1/2 cm, and is composed of 50 to 100 subrings. Each subring is assumed to contain 10^{11} - 10^{12} particles and is azimuthally symmetric. The motion of all particles in a single subring is assumed to be exactly alike so that the movement of the whole group is given by that of a single particle.

Interaction forces are computed between all pairs of subrings which are taken to be infinitesimally thin elements of moving charge for this purpose. To avoid the singularity at small interparticle distances, each subring is considered to be a torus of uniform charge density with typical minor radius of a = 0.5 mm. Electric and magnetic fields at the center of this torus are taken as the bias fields of Laslett[5] and Reiser.[6] This approximation is extended as a continuous function to the surface of the torus. When the distance between two subrings is less than 2a, the finite-sized ring fields are used, while at larger interparticle distances the thin-ring assumption is employed. Retardation effects have been ignored in this analysis, which holds if $\beta_z << 1$.

The multiparticle picture adopted requires a large number of time steps to keep the electron motion accurate in the numerical integration of the equations of motion. Following the motion of real ions where $M_i \gtrsim 2000\ m_e$ would be prohibitively expensive. Poukey, Freeman and Reiser[7] used artificially light ions where M_i = 100 or 400 m_e to study the focusing conditions of ion-loaded electron rings, and the same consideration was adopted for these calculations. Hofmann[8] solved the problem of ring acceleration on a longer time scale by using a different approach based on the Vlasov equation. His geometry and parameters were for the Garching ERA experiment and different from ours.

The squirrel cage (SQC) boundary shown in Figure 2 was simulated by its effective focusing fields. Laslett[5] gives focusing contributions due to the image fields from cylindrical boundaries as

$$\nu^2_{r(\mathrm{Image})} = -4\mu\left[\frac{(1-f)\varepsilon_{1,E}}{(S_E-1)^2} - \beta^2\frac{\varepsilon_{1,M}}{(S_M-1)^2}\right] \qquad (1)$$

$$\nu^2_{z(\mathrm{Image})} = 4\mu\left[\frac{(1-f)\varepsilon_{1,E}}{(S_E-1)^2} - \beta^2\frac{\varepsilon_{1,M}}{(S_M-1)^2}\right] \qquad (2)$$

Here $\mu = \nu/\gamma = N_e r_e/4\pi R\gamma = 4.58 \times 10^{-14} N_e/R_{[cm]}\gamma$, R is the major radius of the electron ring, N_e is the total number of electrons, and f the fraction of ions; the external field index n was assumed to be zero. The image field coefficients are about 1/8 (each) and S_E (S_M) is the ratio of the electric (magnetic) image cylinder radius to that of the beam. For a solid conductor, $S_E = S_M$, and since the two forces are of opposite polarity, there is strong cancellation. Therefore, the suppression of azimuthal image currents

when a SQC is present, i.e., $\varepsilon_{1,M} = 0$, results in improved focusing (which is of particular importance) for the axial motion. In the simulation, any other boundaries were neglected, and the radius of the SQC was varied between 2 and 4 cm compared to a nominal value for R of about 5 cm.

The focusing forces given by equations (1) and (2) increase with distance from the center of the electron ring; but, on a larger scale not accounted for in the approximation that $\varepsilon_{1,E}$ and $\varepsilon_{1,M}$ are nearly constant, they fall off sharply. For simplicity, they were taken as zero beyond some arbitrary constant cutoff distance (see Figure 3) derived from the exact solution (an expansion of Bessel's functions) to the problem of a thin charged ring in a cylindrical box (Smythe[9]). This parameter did not affect the results unless it was smaller than the minor dimensions of the ring. Electrons could still escape to the boundary while ions, which are defocused by the effect, never did.

Parameters for the numerical experiment were chosen on the basis of analytical theory and previous results. Typically, there were 10^{13} electrons in the total ring with kinetic energy of 3.5 MeV, fractional ionization varied from 1 to 5%. The time constant of the coil τ_c was chosen as 5 or 10 ns. This is very short compared to the actual experiment. But the choice of artificially light positive ions ($M_i = 100\ m_e$ or $M_i = 400\ m_e$), permitted a reduction in the time scale and thus a savings in computer time. During the "spillout" process where the downstream mirror is opened, the ring moves essentially with constant radius and with gradually increasing velocity β_z in z-direction. Since β_z is nonrelativistic, the time to travel a distance z may be approximated by

$$t = t_o \left[1 + f \frac{M_i}{\gamma m_e}\right]^{1/2} = t_o \eta \qquad (3)$$

where M_i is ion rest mass ($\gamma_i \approx 1$ in this approximation), and γm_e is the relativistic electron mass. The parameter t_o is the time it would take the electron ring without any ions to travel a given distance. By the same argument, the velocity

$$\beta_z = \beta_{zo} \left[1 + f \frac{M_i}{\gamma m_e}\right]^{-1/2} = \beta_{zo}/\eta \qquad (4)$$

where β_{zo} is the velocity of the electron ring if no ions are present. For f = 0.05, $M_i/m_e = 1836$ (protons), $\gamma = 7.7$, the scaling factor η is 3.59. The use of an artificial mass ratio $M_i/m_e = 100$, reduces this factor to 1.28. The effective computer time is therefore shortened by a factor 3.59/1.28 = 2.8. Conversely, to obtain the actual velocity β_z for protons or any other, heavier ion, one must divide the computer results by the correction factor η of Eq. (3).

3. Results of the Numerical Computations

The computer simulation runs started with a ring of $N_e = 10^{13}$ electrons with the initial conditions t = 0, z = 16.5 cm (center of mirror well). The computer then traced the particles to a final position of z = 70 cm (see Fig. 1).

Additional parameters and the major results of the computer runs are summarized in Table I. The first column shows the (artificial) mass numbers, the second the time constant of the downstream coil. The effective axial betatron frequency due to squirrel-cage focusing only, as calculated analytically from Eq. (2), is shown in the third column. The large number corresponds to a conductor radius of 4 cm, the small number to a radius of 2 cm. It was found that SQC focusing is the dominant effect in the axial motion. The Bennett-Budker self-focusing force due to the factor $f - 1/\gamma^2$ was always less for the two cases (f = 1.25% and f = 5%) considered. Subsequent columns in Table I show the final β_z (at z = 70 cm), the time of travel, the scaling factor η, and the final conditions of the ring. As regards the latter, it was found that in the beginning, the ring as a whole expands somewhat rapidly in cross section and then changes only slowly. The high percentages of electron and ion subrings within cross sectional areas of 1.0 x 1.0 cm^2 and 1.5 x 1.5 cm^2 demonstrate how well the overall integrity of the ion-loaded ring is preserved and that only few particles are lost. It should be noted that an increase in electron number N_e increased the final cross section while a decrease reduced it from the figures given in the table.

The importance of squirrel-cage focusing in our parameter regime is independently verified if one calculates the betatron frequencies from the complete formulas[5,6] (with $\varepsilon_{1,M} = 0$)

$$\nu_r^2 = 1 + \frac{\mu P}{2} + \frac{4\mu R^2}{b(a+b)} \frac{f-(1-\beta^2)}{\beta^2} - 4\mu \frac{(1-f)\varepsilon_{1,E}}{(S_E-1)^2} \qquad (5)$$

$$\nu_z^2 = -\frac{\mu P}{2} + \frac{4\mu R^2}{b(a+b)} \frac{f-(1-\beta^2)}{\beta^2} + \underbrace{4\mu \frac{(1-f)\varepsilon_{1,E}}{(S_E-1)^2}}_{\text{SQC}} \qquad (6)$$

The effect of the external field has been neglected (n = 0) as $\partial B_z/\partial r$ in this region is very small. Minor ring dimensions are 2a, 2b and P = 2 ln[16R/(a+b)]. The SQC term was set at 0.017 or 0.085 (2 cm or 4 cm SQC radius). With f = 5% and the larger SQC focusing value, $\nu_z^2 = 0.073$, $\nu_r^2 = 0.998$. Changing f to 1.25% yields $\nu_z^2 = 0.033$ and $\nu_r^2 = 0.958$. If the smaller SQC value (0.017) is used, $\nu_z^2 = 0.005$ for f = 5% and this provides insufficient focusing, which explains the electron loss in Case 5 of Table I.

The scaling is quite evident when one compares the $M_i = 100\ m_e$, f = 5% figures with $M_i = 400\ m_e$, f = 1.25%. The total ion mass is the same in both cases, and the final β_z is almost identical in good agreement with the scaling law of Eq. (4). In Figure 4, we plotted the kinetic energy versus time for protons ($M_i = 1836\ m_e$, f = 1.09%) by using the data from a run with mass $M_i = 400\ m_e$, f = 5%. The two curves are for two different time constants ($\tau_c = 5$ ns and $\tau_c = 10$ ns) of the downstream coil. Although the time constants are considerably shorter than they would be in practice, the important features are well-demonstrated. In the second case ($\tau_c = 10$ ns), the center of mass of the ring was seen to follow roughly the minimum B_z as the well opens. In the first case with the faster time constant, the ring lags somewhat behind the minimum B_z point due to its inertia, though it still travels the acceleration distance in a shorter time compared to the $\tau_c = 10$ ns case. The most important result is that the kinetic energy of the protons at z = 70 cm is roughly the same in both cases, namely, 3.8 MeV.

One effect observed in the calculations that is of great interest is the center-of-mass motion of the electron and ion subrings. Figure 5 shows the difference Δz of the center of mass of the two

particle species as a function of time for Run 2 (listed in Table I). According to this figure, Δz oscillates, with the ions always staying behind the electrons, and the maximum separation in this case is only 3 mm. No attempt was made to explain the oscillation periods.

4. Conclusions

These numerical simulation experiments demonstrated that an ion-loaded ring, formed in the fast-trapping system of the Maryland ERA, can be safely ejected from the magnetic well without significant losses in particles and major changes in the transverse cross section. Squirrel-cage focusing (suppression of azimuthal image current) is an important prerequisite to achieve successful acceleration in the expanding static magnetic field. The center-of-mass separation between the electron and ion subrings was found to oscillate slightly; however, the amplitude did not exceed more than a few millimeters. It should be noted that these studies assumed axial symmetry of the charge and current distributions. Thus, effects like radial off-centering, negative mass instability and radial electron-ion dipole resonance require separate investigations.

References

1. M. Reiser, IEEE Trans. NS-20, 310 (1973).
2. W. W. Destler, A. Greenwald, D. W. Hudgings, H. Kim, P. K. Misra, M. P. Reiser, M. J. Rhee and C. T. Zorn, Proc. IXth Conf. on High Energy Accelerators, 230 (1974). See also paper by W. W. Destler et al. at this conference.
3. W. Kowalyshyn, J. G. Kalnins, private communication.
4. J. G. Kalnins, H. Kim and J. G. Linhart, IEEE Trans. NS-20, 324 (1973).
5. L. J. Laslett, Technical Reports ERAN 30 (1969) and ERAN 200 (1972), Lawrence Radiation Laboratory, Berkeley, California.
6. M. Reiser, Part. Accel. 4, 239 (1973).
7. J. W. Poukey, J. R. Freeman and M. Reiser, Numerical Studies of Ion-Loaded Rings, to be published in Particle Accelerators.
8. I. Hofmann, Report IPP 0/21, Max-Planck-Institut f. Plasmaphysik, Garching (W. Germany), February 1974.
9. W. R. Smythe, Static and Dynamic Electricity, Third Edition, McGraw Hill 1968, p. 199.

*Research supported by the National Science Foundation and the University of Maryland Computer Science Center.

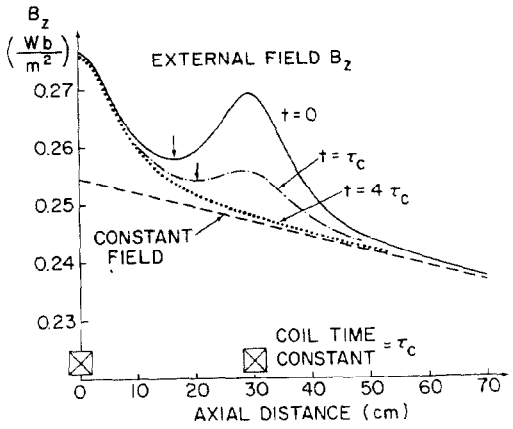

Fig. 1. Axial magnetic field.

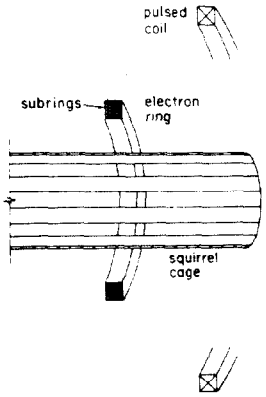

Fig. 2. Schematic diagram of electron ring with inner squirrel cage and one of the pulsed coils shown.

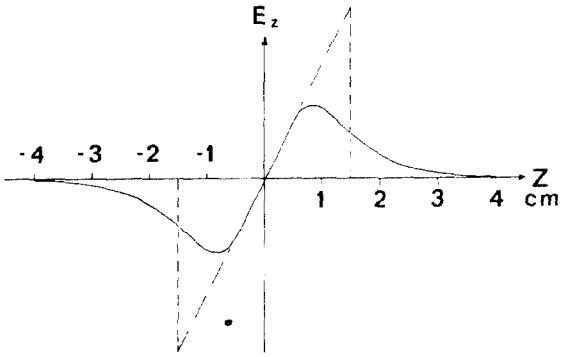

Fig. 3. Axial electric field due to thin ring charge in cylindrical box. Dotted curve is approximation used in code.

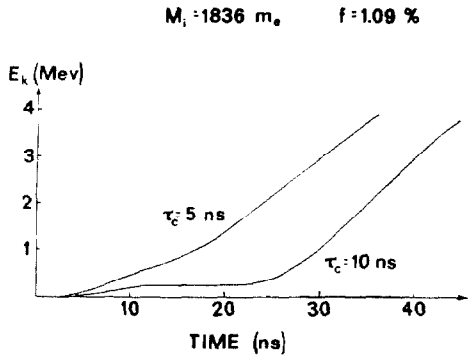

Fig. 4. Energy versus time for Runs 2 and 3 extrapolated to proton mass.

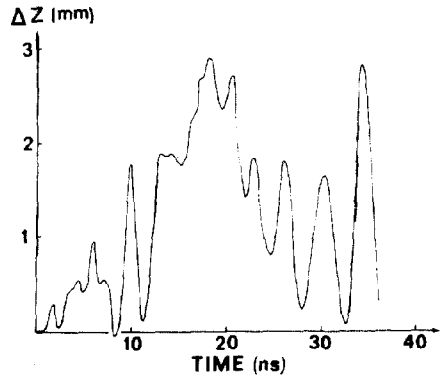

Fig. 5. Relative spacing between center of mass of ion distribution and center of mass of electron distribution versus time for Run 2.

Table I

Run #	Ion mass $\times m_e$	τ_c (ns)	ν_z^2 SQC	f %	β_z final	t_f† (ns)	η	% Electrons in square cross section, Z = 30 cm, 1x1 cm^2	% Electrons in square cross section, Z = 30 cm, 1.5x1.5 cm^2	% Electrons in square cross section, Z = 70 cm, 1x1 cm^2	% Electrons in square cross section, Z = 70 cm, 1.5x1.5 cm^2	% Ions in square cross section, Z = 30 cm, 1x1 cm^2	% Ions in square cross section, Z = 30 cm, 1.5x1.5 cm^2	% Ions in square cross section, Z = 70 cm, 1x1 cm^2	% Ions in square cross section, Z = 70 cm, 1.5x1.5 cm^2
1	400	5.0	0.085	1.25	.131	26.4	1.29	80	100	75	90	100	100	70	100
2	400	5.0	0.085	5.0	.091	35.8	1.91	70	90	60	90	70	90	70	85
3	400	10.0	0.085	5.0	.091	45.4	1.91	80	100	70	90	80	90	70	90
4	100	5.0	0.085	5.0	.136	25.2	1.29	90	100	90	100	90	90	55	70
5	100	5.0	0.017	5.0	*	*	1.29	75	80	*	*	85	95	*	*

† t_f = time of travel to reach Z = 70 cm position.

*Case 5 stopped when particle loss became excessive before the final position (Z = 70 cm) was reached.

Other tests performed:

(1) Smaller subrings had no effect.

(2) No SQC focusing led to 40% electron loss for f = 5%.

(3) Change of spacing between pulsed coils had small effect.

(4) Increasing number of particles in ring increased minor dimensions.